J MATER SCI 41 (2006) 2577–2580

Electron beam-induced formation of nanosized α-Fe crystals

W. ZHANG*
High Voltage Electron Microscopy Station, National Institute for Materials Science, 3-13 Sakura, Tsukuba 305-0003, Japan
E-mail: zhang.wei@nims.go.jp

M. SHIMOJO
High Voltage Electron Microscopy Station, National Institute for Materials Science, 3-13 Sakura, Tsukuba 305-0003, Japan; Precision and Intelligence Laboratory, Tokyo Institute of Technology, 4259 Nagatsuta, Midori, Yokohama, 226-8503, Japan

M. TAKEGUCHI, K. FURUYA
High Voltage Electron Microscopy Station, National Institute for Materials Science, 3-13 Sakura, Tsukuba 305-0003, Japan

Focused electron beam induced chemical vapor deposition was performed in a scanning electron microscope with a field emission gun using a precursor of iron carbonyl. Due to the longer deposition time and higher gas pressure than those of our previous electron beam-induced deposition method, a new type of deposition occurred. A large amount of nanosized crystals were produced around the focused beam irradiation point on a carbon substrate at room temperature. The nanocrystals were systematically characterized using transmission electron microscopy with electron energy loss spectroscopy (EELS), and were identified to be single crystals of α-Fe. © *2006 Springer Science + Business Media, Inc.*

1. Introduction

The fabrication of nanosized magnetic structures is currently receiving much interest because of its potential application in nanotechnology as well as for the fundamental understanding of nanomagnetics [1–3]. Electron beam-induced deposition (EBID) using metal carbonyl precursors is a promising technique for nanofabrication and has been extensively studied. Tanaka *et al.* [4] and Mitsuishi *et al.* [5] fabricated nanodots, the sizes of which are less than 5 nm, by EBID. Also, two- and three-dimensional structures, e.g., nanowires, nanofigures and nanorods have been synthesized [6–8]. However, their applications seem to be limited, since most of these structures are amorphous phases or nanocrystals distributed in an amorphous carbonaceous matrix, and the deposits usually contain a large quantities of carbon atoms in addition to the metal ones. Although crystallization can be achieved through post heat-treatments [3], it is difficult to obtain nanosized single crystals by this method.

In the present paper, we report the formation of a large amount of nanosized α-Fe single crystals. This suggests the possibility for fabricating crystalline, especially single-crystalline, nanostructures at room temperature directly by EBID. Such a nanostructure may be potentially useful for bottom-up self-assembly in micro- and nanofabrication.

2. Experimental procedures

A JEOL JSM-7800UHV field emission gun scanning electron microscope (SEM), operated at 30 kV was used for EBID at a beam current of 8×10^{-10} A. The base pressure of the specimen chamber was 2×10^{-6} Pa. Iron pentacarbonyl ($Fe(CO)_5$) was used as a precursor. Precursor vapor was introduced to the chamber though a nozzle installed on the SEM. Carbon micro-grid films were used as substrates.

---

*Author to whom all correspondence should be addressed.

0022-2461 © *2006 Springer Science + Business Media, Inc.*
DOI: 10.1007/s10853-006-7783-1

In our previous electron beam-induced deposition (EBID), a 3-nanodot array on the substrate was made by focused electron beam irradiation for 60 s under about 7×10^{-5} Pa of the pressure gas in the chamber [3]. Due to longer deposition time (1000 s) and higher gas pressure (1.2×10^{-4} Pa) in the present EBID, a new type of deposition on the substrate was produced around the focused beam irradiation point (deposited nanodot) at room temperature.

Microstructures of the deposits were observed using a transmission electron microscope (TEM), JEOL JEM-3000F, attached with an electron energy loss spectroscopy (EELS) apparatus at room temperature, operated at 300 kV.

3. Results and discussion

A focused electron beam was irradiated on the substrate, and a nanodot was formed on the substrate as conventional electron beam-induced deposition. Around the nanodot on the substrate, a large amount of nanosized crystals were formed, a SEM image of which is shown in Fig. 1. The shape of each crystal resembles a cube.

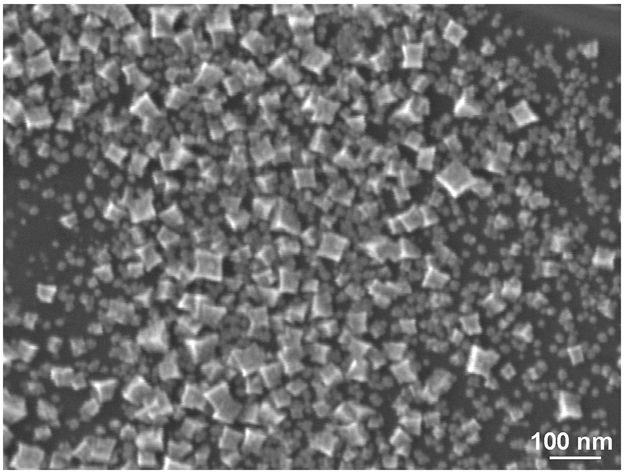

Figure 1 SEM image of nanosized α-Fe crystals.

Figs 2a and b show a bright-field TEM image and corresponding electron diffraction pattern, respectively. It was found that these crystals possessed random crystallographic orientations. By indexing the diffraction pattern, such crystals were identified to be bcc α-Fe. There exist two additional weak diffraction halos that are from the amorphous carbon substrate and iron oxides (Fe_3O_4 or Fe_2O_3), respectively. The formation of the latter is considered to be due to the exposure to the air during the transportation from the SEM to the TEM.

Such analysis was further verified by the following EELS analyses, as shown in Figs 3 and 4. Fig. 3 shows an EELS spectrum taken from the deposited nanosized α-Fe crystals on the carbon substrate. A broad carbon σ^* edge appears in the EELS spectrum, which is a typical feature of the EELS spectrum from amorphous carbon. The small oxygen peak in the EELS spectrum came from the aforementioned effect. Meanwhile one can see the sharp Fe EELS peaks $L_{2,3}$ in the spectrum. Fig. 4 shows a zero-loss image and a corresponding Fe elemental map. One can see that in the Fe elemental mapping, Fe profile is overlapped well with the crystal morphology in the zero-loss image. Each crystal is numbered in Fig. 4a.

Fig. 5 shows a typical HREM image of a crystal. The edges seem to consist of $\{100\}$ planes. The top-left and bottom-left insets are a local enlargement of the boxed area and corresponding Fourier diffractogram. The two characteristic planes $(110)_{\alpha\text{-Fe}}$ and $(\bar{1}10)_{\alpha\text{-Fe}}$ are labeled, the spacings of which are about 0.20 nm. According to the electron diffraction, EELS and HREM analyses, it is suggested that the crystals are single crystal α-Fe.

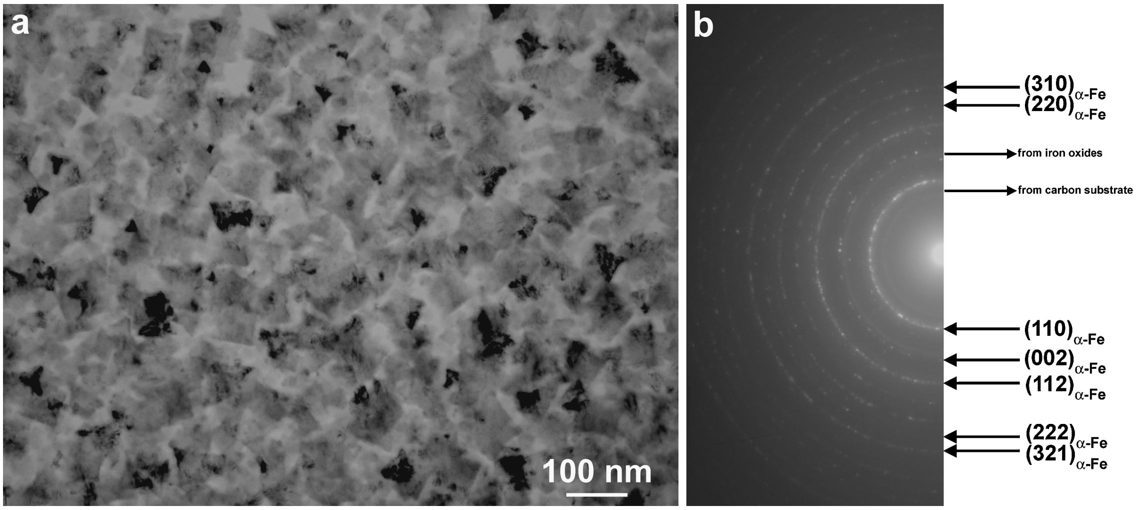

Figure 2 Bright-field TEM image (a) and corresponding electron diffraction pattern (b) of the nanosized α-Fe crystals.

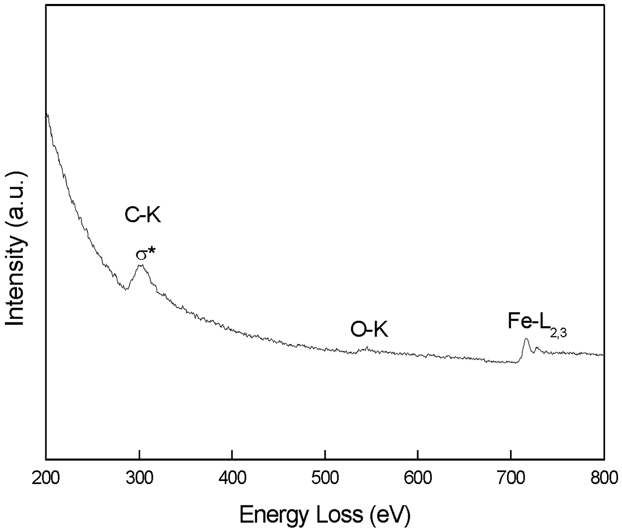

Figure 3 EELS spectrum of the deposited nanosized α-Fe crystals on the carbon substrate.

Obviously, the formation of α-Fe crystals was closely associated with the decomposition of iron carbonyl molecules under the focused electron beam irradiation. Also some $Fe(CO)_5$ molecules were adsorbed on the surface of the substrate. By the irradiation of the incident focused electron beam, the precursor molecules were dissociated into non-volatile and volatile components. The volatile materials are evacuated by the vacuum system, while the non-volatile ones accumulate to form the deposition on the substrate.

The decomposition of $Fe(CO)_5$ has been investigated in several studies. It was reported that $Fe(CO)_4$–(CO) bond dissociation energy was 2.38 eV, whereas the second dissociation energy $Fe(CO)_3$–(CO) was reduced to less than 0.61 eV [9]. Lewis *et al* reported [10] that Fe was rapidly formed following the removal of the first CO. It was verified that only Fe and $Fe(CO)_5$ without other Fe-containing fractions were detected on the substrate [11–13]. Koops *et al.* reported that the threshold energy to dissociate the C–O bond was about 12 eV [14]. It is well known that the secondary electrons emitted from the substrate with energies ranging from 0 to 50 eV, play a very important role in the electron beam induced deposition process [6]. Therefore, in the area of electron beam irradiation, Fe, C and O atoms/ions can be formed due to the dissociation of $Fe(CO)_5$ by the effect of secondary electrons.

The formed Fe, C and O atoms/ions deposit in part at the beam irradiation position, and small fractions of them may be deposited around the irradiation position. This might be due to the local temperature increase by the electron beam irradiation or sputtering effect by the high-energy electron beam. Some molecules above the substrate within the electron beam may be decomposed and deposited around the irradiation position on the substrate though the dissociation cross section of the primary electron beam is small. Kunz and Mayer [15] also reported that an autocatalytic decomposition of $Fe(CO)_5$ and the formation of an Fe film occurred after the unfocused electron beam irradiation was stopped once the Fe film was formed as a nucleation step, though the experimental conditions, such as beam energy and substrate temperature, were different from our study. In our experiments, a similar process may be considered to occur for the formation of Fe nano-crystals, though further studies are necessary to clarify the mechanism. That is, atoms or tiny clusters of Fe may be deposited around the irradiation position on the substrate, these Fe atoms act as nucleation sites, and Fe crystals grow due to such an autocatalytic decomposition.

In short, our work may open a new route that monocrystalline nanosized metal particles can be fabricated just simply by using focused electron beam-induced

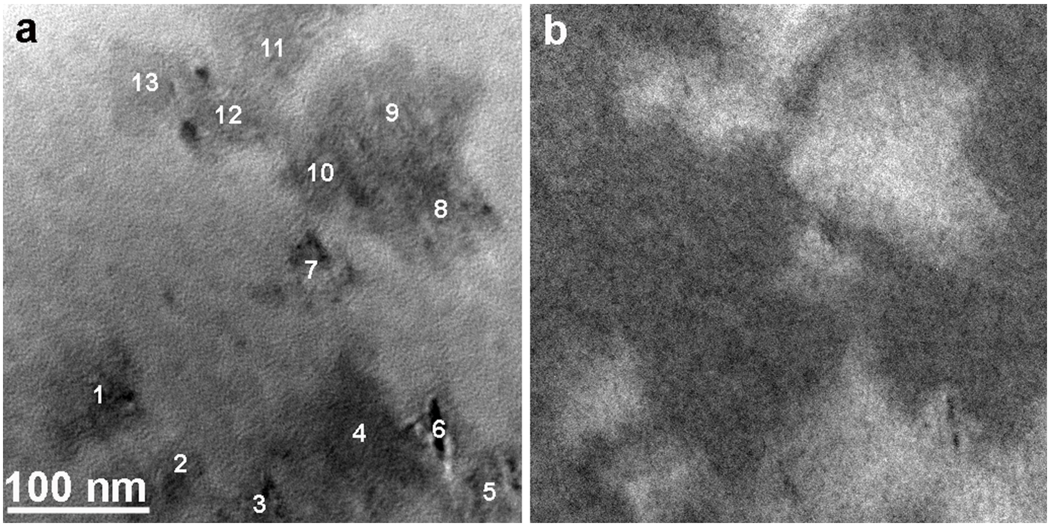

Figure 4 Zero-loss image (a) and Fe EELS mapping (b) of Fe nano-crystals on carbon substrate.

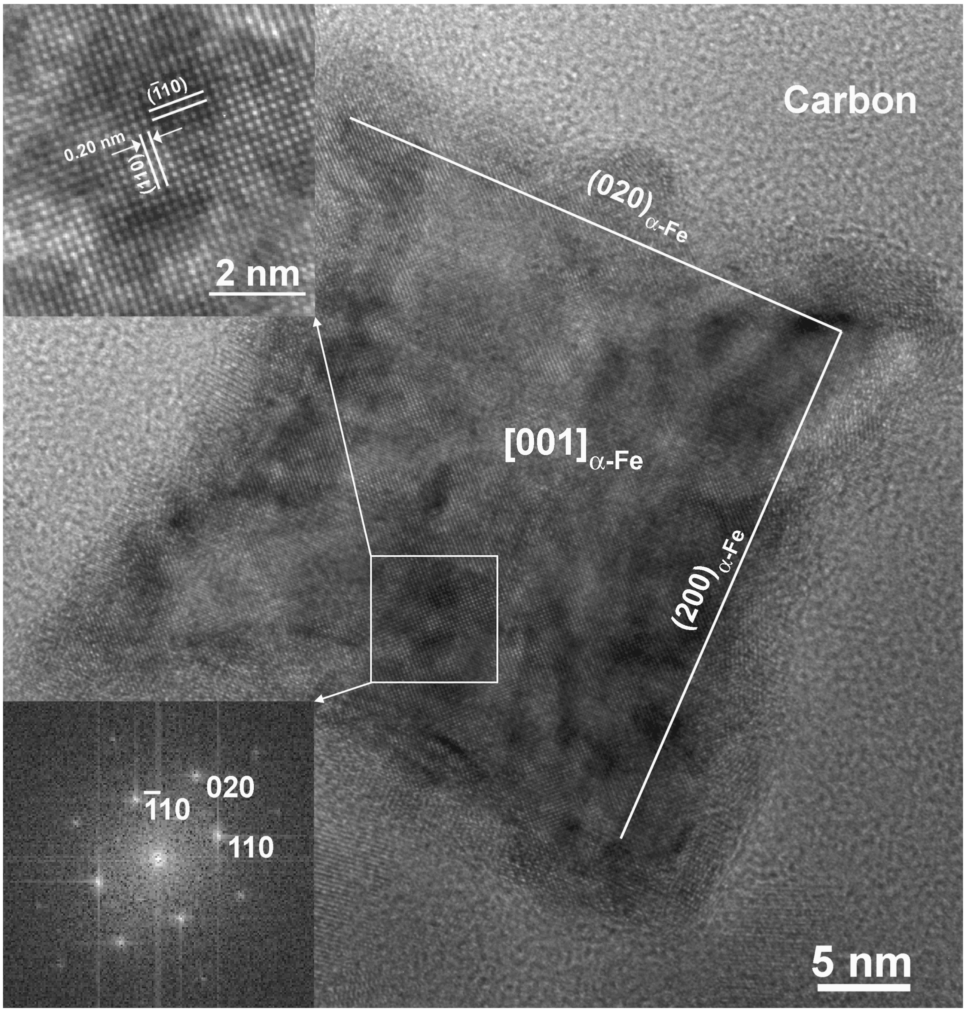

Figure 5 HREM image of a typical nanosized α-Fe crystal.

deposition at room temperature using metalorganic precursors.

4. Conclusions

Nanosized α-Fe single-crystals were fabricated on a carbon substrate by focused electron beam-induced deposition using $Fe(CO)_5$ as a precursor. This is a novel route to deposit such isolated nano-crystals at room temperature.

Acknowledgements

One of the authors (WZ) would like to thank Drs. R.C. Che and Z.Q. Liu for their help, Drs. J.C. Rao, F.M. Chu and G.Q. Xie for some valuable discussions.

References

1. S. W. JUNG, W. I. PARK, G. C. YI and M. KIM, *Adv. Mat.* **15** (2003) 1358.
2. D. G. SHCHUKIN, I. L. RADTCHENKO and G. B. SUKHORUKOV, *J. Phys. Chem. B* **107** (2003) 86.
3. M. SHIMOJO, M. TAKEGUCHI, M. TANAKA, K. MITSUISHI and K. FURUYA, *Appl. Phys. A* **79** (2004) 1869.
4. M. TANAKA, M. SHIMOJO, K. MITSUISHI and K. FURUYA, *ibid.* **78** (2004) 543.
5. K. MITSUISHI, M. SHIMOJO, M. HAN and K. FURUYA, *Appl. Phys. Lett.* **83** (2003) 2064.
6. N. SILVIS-CIVIDJIAN, C. W. HAGEN, P. KRUIT, M. A. J. VAN DER STAM and H. B. GROEN, *ibid.* **82** (2003) 3514.
7. I. UTKE, A. LUISIER, P. HOFFMANN, D. LAUB and P. A. BUFFAT, *ibid.* **81** (2002) 3245.
8. K. UEDA and M. YOSHIMURA, *Thin Solid Films* **464/465** (2004) 331.
9. P. C. ENGELKING and W. C. LINEBERGER, *J. Am. Chem. Soc.* **101** (1979) 5569.
10. K. E. LEWIS, D. M. GOLDEN and G. P. SMITH, *ibid.* **106** (1984) 3905.
11. J. PHILLIPS and J. A. DUMESIC, *Appl. Surf. Sci.* **7** (1981) 215.
12. J. S. FOORD and R. B. JACKMAN, *Chem. Phys. Lett.* **112** (1984) 190.
13. J. R. SWANSON, C. M. FRIEND and Y. J. CHABAL, *J. Vac. Sci. Technol. A* **6** (1988) 770.
14. H. W. P. KOOPS, A. KAYA and M. WEBER, *J. Vac. Sci. Technol. B* **13** (1995) 2400.
15. R. R. KUNZ and T. M. MAYER, *ibid.* **6** (1988) 1557.